Magneto-optic constants of hcp and fcc Co films

R. M. Osgood III, K. T. Riggs,* Amy E. Johnson,† J. E. Mattson,‡ C. H. Sowers, and S. D. Bader
Materials Science Division, Argonne National Laboratory, Argonne, Illinois 60439
(Received 10 February 1997)

We tabulate the wavelength dependence of the complex magneto-optic constants for epitaxial fcc (001) and hcp $(11\bar{2}0)$ Co films with the magnetization along two different in-plane crystallographic directions. The magneto-optic constants of epitaxial hcp Co films are strongly dependent on crystallographic direction for the same sample, while those of epitaxial fcc Co films are not, as anticipated from the trends in the magnetic anisotropy due to the spin-orbit interaction. Our results for (i) the anisotropic magneto-optic constants, (ii) the magnetic anisotropy, and (iii) the indices of refraction, are compared to other studies of Co. [S0163-1829(97)01729-3]

I. INTRODUCTION

The magneto-optic Kerr effect (MOKE) has been shown to play an important role in the analysis of surface magnetism.[1] However, widely different magneto-optic constants for Co have been reported in the literature. For example, the classic survey in the visible region of the magneto-optic properties of Fe, Co, and Ni by Krinchik and Artem'ev (KA) in 1968 used polycrystalline plates.[2] More recently, Qiu, Pearson, and Bader[3] measured the Kerr ellipticity in the longitudinal geometry at the He-Ne wavelength as a function of thickness for epitaxial Co overlayers on Cu (100) and Cu(111), and for Co/Cu superlattices, observing both monotonic and nonmonotonic behavior, respectively, as a function of layer thickness. These authors fitted this data in order to obtain the magneto-optic constants. Most recently, Weller *et al.*[4] determined the *polar* Kerr rotation and ellipticity of epitaxial Co films with different crystallographic orientations. These studies exhibit qualitative and quantitative differences that are extremely interesting to pursue in order to develop a more complete understanding of magneto-optics and its origins. Here we use the standard definition of the magnetization components: the polar component lies out-of-plane in the plane of incidence of the light, while the longitudinal component lies also in the plane of incidence of the light, but in the plane of the sample.

The great resurgence of interest in magneto-optics is coupled to our understanding of the anomalous Hall effect and the dielectric tensor of ferromagnetic metals in general. The complex magneto-optic constant $Q=Q'+iQ''$ provides a measure of the size of the off-diagonal component of the dielectric tensor, as discussed by Bolotin and Sokolov, and can be related to the Hall constant (note that we are using the convention $e^{+i\omega t}$ for the time dependence):[5]

$$in_0^2 Q=\frac{4\pi\sigma_{yz}}{i\omega}, \tag{1}$$

$$R_H=\frac{\rho_{yz}}{H_z}=\frac{-\sigma_{yz}}{\sigma_{zz}^2+\sigma_{yz}^2}\frac{1}{H_z}\cong\frac{4\pi n_0^2 Q}{\omega(n_0^2-1)^2}, \tag{2}$$

where ω is the frequency of light, the magnetic field H_z is applied along the z direction, and ρ_{yz} (σ_{yz}) is the off-diagonal component of the resistivity (conductivity) tensor. We have expanded to first order in Q, and we have written

$$n_0^2=1+\frac{4\pi\sigma_{zz}}{i\omega}, \tag{3}$$

which attributes all of the dielectric response to conduction electrons. The parameter Q can therefore be thought of as a high-frequency Hall constant, with an applied magnetic field H_z replaced by an effective magnetic field proportional to the magnetization **M**, much as is done in the case of the anomalous Hall effect.[6]

The spin-orbit coupling is what connects the magnetization of the sample to the lattice and therefore causes magnetic anisotropy. Spin-orbit coupling causes preferential absorption of left- over right-handed light and therefore is responsible for the Kerr effect as well. Q therefore should depend on the direction of **M** with respect to the crystal axes, and since the magnetic anisotropy is larger for a uniaxial material than for a cubic material, the anisotropy in Q should be larger in a hexagonal close-packed (hcp) structure than in a face-centered-cubic (fcc) structure.[4] In addition, such an anisotropy in Q might explain the discrepancies observed between Q values reported in the literature.

Weller *et al.*[4] have shown that the magneto-optic response is different for **M** along the $[11\bar{2}0]$ and [0001] directions of epitaxial hcp Co (no anisotropy was observed for epitaxial fcc Co with different out-of-plane orientations). The samples they used had one of these two directions normal to the sample surface, so that they always used the polar Kerr effect to measure the magneto-optic properties. One is naturally lead to the question: are the differences in the magneto-optic response they observed truly due to an anisotropy in Q, or are they due to differences between the optical properties of the different samples? In order to verify the Q anisotropy of hcp Co, we have conducted similar experiments on a sample of hcp Co with *in-plane* $[11\bar{2}0]$ and [0001] directions, so that the anisotropy in the magneto-optic response of the *same sample* can be measured by a simple in-plane rotation. We verify the magneto-optic anisotropy observed by Weller *et al.* and report energy-dependent values of Q' very similar to his. In addition, we have obtained Q values of an epitaxial fcc Co sample with **M** along the in-plane [001] and [011]

TABLE I. Magnetic anisotropy coefficients for the hcp and fcc samples.

Sample	K_1 (ergs/cm^3)	K_2 (ergs/cm^3)
hcp Co	$3.4\pm0.4\times10^6$	$1.5\pm0.4\times10^6$
fcc Co	$-0.8\pm0.1\times10^6$	

directions, confirming the observation of Weller *et al.* that no significant anisotropy in Q exists in this case. Finally, we obtain very similar optical constants to those reported by KA.[2] The anisotropy in Q we observe cannot explain discrepancies between Q values reported in the literature, and we discuss the possibility of these discrepancies being due to a thin oxide layer on the sample's surface.

II. THEORETICAL BACKGROUND

In this article, we use the convention of Metzger *et al.*,[7] who used a linear basis to describe the magneto-optic effects. Metzger *et al.* gave expressions for the magneto-optic effects up to second order in Q and for any general magnetization direction.[7] Metzger *et al.* defined the magneto-optic effects in terms of the effect of the sample on light polarized either parallel (p) or perpendicular (s) to the plane of incidence. In the case of normal incidence, a distinction is made between the Kerr rotation and Kerr ellipticity for s- and p-polarized light:

$$s\text{-polarized: } \frac{in_0Q}{n_0^2-1}=\theta_k^s+i\epsilon_k^s, \tag{4}$$

$$p\text{-polarized: } \frac{-in_0Q}{n_0^2-1}=\theta_k^p-i\epsilon_k^p, \tag{5}$$

where $n_0=n-ik$ is the index of refraction (n and k are positive numbers) and $\theta_k^{p,s}$, $\epsilon_k^{p,s}$ are real numbers that give the amount of (p,s) rotation and ellipticity, respectively. In the limit of normal incidence, of course, s- and p-polarized light are identical, so that θ_k^s and θ_k^p represent opposite senses of rotation.

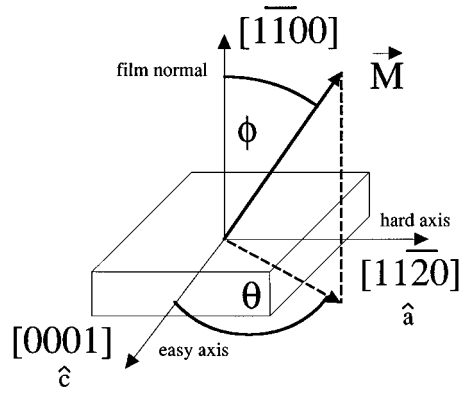

FIG. 1. Crystallographic axes for the hcp Co sample. **M** lies in the plane of the sample at an angle θ from the [0001] direction. Were **M** to be out of plane, it would lie at an angle ϕ from the out-of-plane [1100] direction.

The fact that the imaginary part of n_0 is negative is opposite to the convention used in Qiu, Pearson, and Bader,[3] but agrees with the convention used by Metzger *et al.* and Reim and Schoenes.[7,8] This convention also influences the sign of the factors Q'' and $\epsilon_k^{p,s}$.

Reim and Schoenes,[8] as well as Weller *et al.*,[4] have defined the rotation and ellipticity for normal incidence using a circular basis. We label the rotation and ellipticity used by Reim and Schoenes θ_k and ϵ_k, respectively. ϵ_k is nonzero due to selective absorption of one handedness over another and is therefore the real part of the difference between reflectivities for left- and right-circularly polarized light, while θ_k is nonzero due to the phase delay of one handedness with respect to another and is therefore the imaginary part of the difference between reflectivities for left- and right-circularly polarized light. Mathematically, these relationships are expressed as follows:

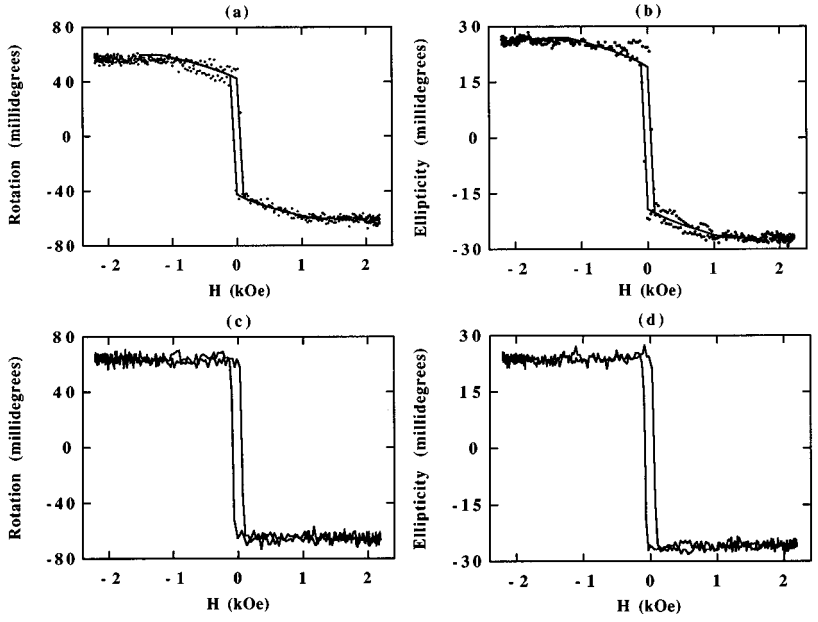

FIG. 2. MOKE hysteresis loops from the fcc Co sample at 1.5 eV. The dots represent the experimental data; the solid line is a fit to the data described in the text. (a), (b) is rotation (ellipticity) for H along the hard ([001]) direction; (c), (d) is rotation (ellipticity) for H along the easy ([011]) direction.

$$\epsilon_k = -\mathrm{Re}\left(\frac{r_+ - r_-}{r_+ + r_-}\right), \tag{6}$$

and

$$\theta_k = -\mathrm{Im}\left(\frac{r_+ - r_-}{r_+ + r_-}\right), \tag{7}$$

where $n_{+,-}$ are indices of refraction for left- and right-circularly polarized waves and $(1-n_{+,-})/(1+n_{+,-}) = r_{+,-}$ are the Fresnel reflectivities for left- and right-circularly polarized waves at normal incidence.

One simplifies these expressions to yield

$$\epsilon_k = -\mathrm{Re}\left(\frac{n_+ - n_-}{n_+ n_- - 1}\right), \tag{8}$$

$$\theta_k = -\mathrm{Im}\left(\frac{n_+ - n_-}{n_+ n_- - 1}\right), \tag{9}$$

from which one obtains

$$\epsilon_k = -\mathrm{Re}\left(\frac{n_0 Q}{n_0^2 - 1}\right), \tag{10}$$

$$\theta_k = -\mathrm{Im}\left(\frac{n_0 Q}{n_0^2 - 1}\right), \tag{11}$$

yielding

$$\theta_k - i\epsilon_k = \frac{i n_0 Q}{n_0^2 - 1}, \tag{12}$$

which agrees with the expression for p-polarized light from Metzger, except for an overall minus sign. Our definition of Q will therefore be the negative of that obtained using the formulas of Reim and Schoenes; however, the relationship between Q' and Q'' will be the same as for Reim and Schoenes.

III. EXPERIMENT

A. The Samples

Two epitaxial samples were prepared for the analysis of the anisotropy in Q: and hcp and fcc Co film. The fcc Co film is 500-Å thick and was deposited directly onto (100)-oriented MgO at 600 °C. A 20-Å-thick cover layer of Cr was deposited on top at 200 °C. The hcp Co film was grown by depositing a 500-Å-thick Co layer onto an MgO(110) substrate with a 200-Å-thick Cr base layer and 15-Å-thick Cr cap layer. The base layer was deposited at 600 °C and the cap and Co layers were deposited at 300 °C.

A polycrystalline Co film with a nominal thickness of 1200 Å was sputter deposited at room temperature onto unoriented sapphire. This Co film was used as a standard for obtaining the indices of refraction of polycrystalline Co. These indices of refraction, not the literature values, were used for the subsequent determination of Q.

The fcc Co film was confirmed via x-ray diffraction to be (100)-oriented with a rocking curve full width at half maximum (FWHM) of 1.3°. The hcp Co film was also epitaxial, with a rocking curve FWHM of 2.4° and an out-of-plane $[1\bar{1}00]$ orientation. The Cr base layer for this sample was (211)-oriented and served as a buffer layer for the subsequent Co growth.

B. The magnetic anisotropy of the Co samples

The magnetic anisotropy constants $K_{1,2}$ were measured in order to confirm the expectation that the (100)- and (110)-oriented samples had four- and twofold magnetic anisotropy, respectively. $K_{1,2}$ were found by simulating MOKE hysteresis loops. These anisotropy coefficients are given in Table I. The anisotropy energy density for the fcc sample is given by

$$E/V = K_1(\alpha_x^2\alpha_y^2 + \alpha_y^2\alpha_z^2 + \alpha_z^2\alpha_x^2) + K_2\alpha_x^2\alpha_y^2\alpha_z^2, \tag{13}$$

where $K_{1,2}$ are the first- and second-order anisotropy coefficients, respectively, and α_i is the direction cosine from the ith crystal axis. K_2 could not be determined for this sample because $\alpha_z = 0$, since **M** was confined to the plane. The anisotropy energy density for the hcp sample is given by

$$E/V = K_1\sin^2\theta + K_2\sin^4\theta, \tag{14}$$

where K_1 and K_2 are the first- and second-order anisotropy coefficients, respectively, and θ is the angle between **M** and the easy axis [the (0001) or c axis] (see Fig. 1). Note that no crystalline anisotropy has been assumed to exist in the basal plane (the shape anisotropy adds a ϕ-dependent term, where ϕ, contrary to tradition, is the angle between **M** and the $(1\bar{1}00)$ out-of-plane direction). The two anisotropy coefficients were determined by fitting hysteresis loops measured from the hcp sample along the in-plane easy and hard axes, and averaging these results with those obtained using Brillouin light scattering (Ref. 9 contains results from the same

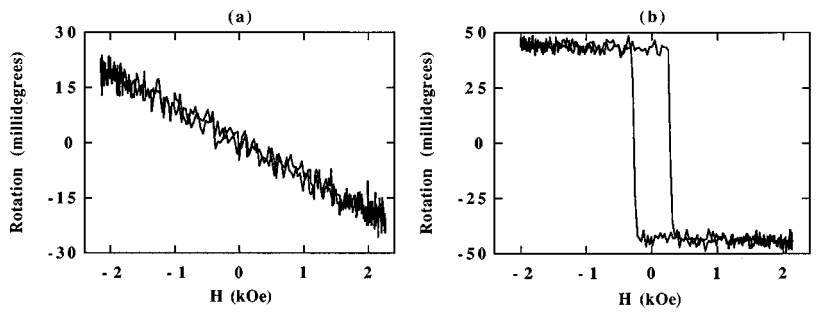

FIG. 3. Hysteresis loops measured by MOKE (Kerr rotation) from the hcp Co sample for H along the (a) $[11\bar{2}0]$ (hard) and (b) [0001] (easy) direction at 1.7 eV.

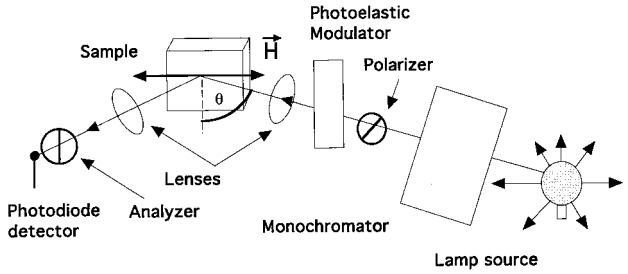

FIG. 4. Schematic diagram of Kerr spectrometer. Light from a lamp source passes through a monochromator, a polarizer, a 50 kHz photoelastic modulator, and is focused onto the sample. The reflected light acquires a magneto-optic rotation and ellipticity. The reflected light is expanded through an output lens and passes through an analyzing polarizer oriented 45° to the input polarizer. Finally, the beam reaches a photodiode detector. The angle of incidence is 36° from the normal. The dc and ac components of the detected signal are amplified separately and sent to a divider circuit connected to the input of a lock-in amplifier. H is applied in the plane of the sample and in the plane of the incident and reflected light.

sample).[9] These anisotropy coefficients are close to those previously reported by Weller *et al.* using torque magnetometry,[4] although the fcc sample's K_1 was larger than that reported in Ref. 4 by about 32%. This discrepancy might be explained by differences between the strain anisotropy in our samples (the samples used by Weller *et al.* had a different seed layer present).

The fourfold symmetry of the fcc sample was verified with MOKE measurements, where the hysteresis loops displayed shapes typical for fourfold symmetry (see Fig. 2 for hysteresis loops measured at a representative energy of 1.5 eV): the hard axis [Figs. 2(a) and 2(b)] had a slow approach to saturation (which occurred at a field of roughly 1.1 kOe) after a sharp transition at small (~50 Oe) fields, while the easy axis [Figs. 2(c) and 2(d)] is saturated at a much smaller field. The data displayed in Figs. 2(a) and 2(b) (H parallel to the hard axis) have been fitted assuming **M** to lie always in its equilibrium position; i.e., assuming magnetization reversal via coherent rotation, so that the coercivity of the loop is determined entirely by the anisotropy field of the sample. The other input parameters to the fit are the anisotropy constant, the Q value, and the index of refraction obtained from the polycrystalline Co sample. The anisotropy field measured by MOKE agrees with that obtained by a superconducting quantum interference device (SQUID) magnetometer to within 10% (this gives the error bar in Table I).

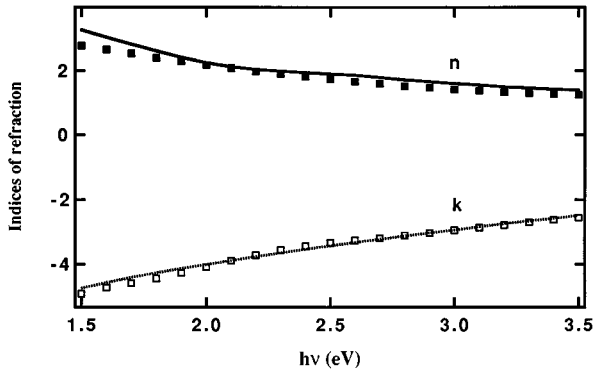

FIG. 5. Indices of refraction as a function of photon energy ($h\nu$) obtained from the polycrystalline Co sample (boxes) and those used by KA (curves) (Ref. 2).

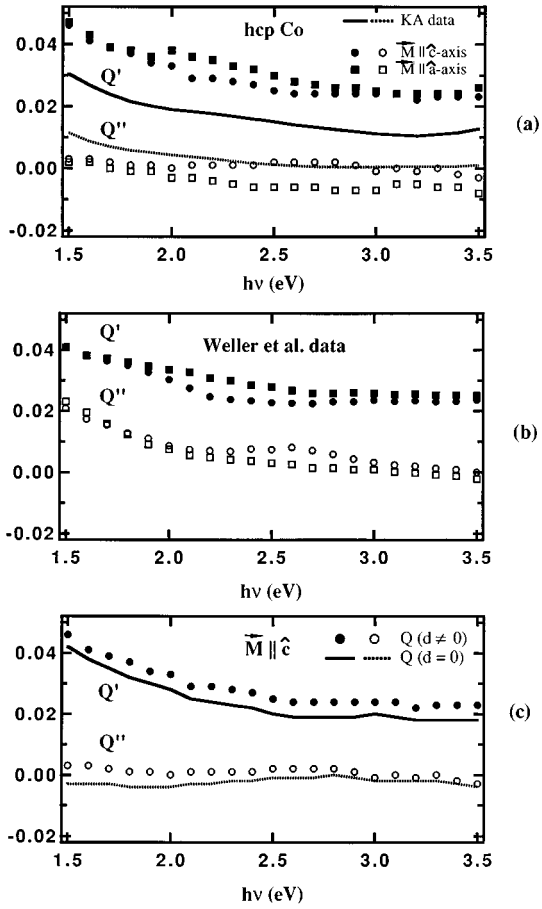

FIG. 6. Q values as a function of photon energy ($h\nu$) for the hcp Co sample. In panel (a), the solid (clear) boxes are Q' (Q'') for **M** along the in-plane [1120] ($\hat{a}$ axis); the solid (clear) circles correspond to **M** along the in-plane [0001] ($\hat{c}$ axis); see Fig. 1 for the definition of these axes. For the latter two data sets, indices of refraction were obtained from the polycrystalline Co sample, as described in the text. The solid (dotted) lines are Q' (Q'') from KA (Ref. 2) (indices of refraction from the same source). Panel (b) was obtained from the data by Weller *et al.*, (Ref. 4), with indices of refraction obtained from KA. Panel (c) represents $\mathbf{M}\|\hat{c}$ with Q derived from Eq. (18) [circles as in (a) above] and with capping layer thickness $d=0$.

Figure 3 displays hysteresis loops measured by MOKE (Kerr rotation) from the epitaxial hcp Co sample for the applied field along the (a) [1120] (hard) (b) [0001] (easy) direction at a representative energy of 1.7 eV. **M** could not be saturated with the available field (H) along the hard axis, so it was necessary to extrapolate the rotation and ellipticity to the saturation field obtained with SQUID magnetometry. K_1 and K_2 for the epitaxial hcp sample were determined by fitting the SQUID hysteresis loops.

C. The magneto-optic constants

The energy dependence of the magneto-optic response was measured with a Kerr spectrometer that uses a photoelastic modulator (PEM) as a means of obtaining a signal linear in both the ellipticity and rotation, and is sketched in Fig. 4. The light from a Xe are discharge lamp was passed through a monochromator,[10] then a polarizer oriented 45° to the plane of incidence, through a PEM, and through a lens onto the sample. The reflected light passed through a lens, through an analyzer, and into a photodiode detector. If we use the Jones matrix formalism in the $\binom{p}{s}$ basis,[11] we may write the detected intensity as

$$I=\left|\begin{pmatrix}0 & \epsilon\\ \epsilon & 1\end{pmatrix}\begin{pmatrix}r_{pp} & r_{ps}\\ r_{sp} & r_{ss}\end{pmatrix}\begin{pmatrix}1 & 0\\ 0 & e^{i\phi}\end{pmatrix}\frac{1}{\sqrt{2}}\begin{pmatrix}1\\ 1\end{pmatrix}\right|^2, \tag{15}$$

where $\left(\begin{smallmatrix}0 & \epsilon\\ \epsilon & 1\end{smallmatrix}\right)$ represents the analyzer (now set $\epsilon=4°$ from eliminating the p polarization), $\left(\begin{smallmatrix}1 & 0\\ 0 & e^{i\phi}\end{smallmatrix}\right)$ represents the PEM, $\left(\begin{smallmatrix}r_{pp} & r_{ps}\\ r_{sp} & r_{ss}\end{smallmatrix}\right)$ represents the sample, and $1/\sqrt{2}\left(\begin{smallmatrix}1\\ 1\end{smallmatrix}\right)$ represents the polarization state of the light exiting the monochromator, polarized 45° to the plane of incidence. Multiplying this out, and neglecting terms of order r_{sp}^2, $r_{sp}\epsilon$, and ϵ^2, we get

$$\begin{aligned} I&=\frac{1}{2}\,|r_{sp}+\epsilon r_{pp}+r_{ss}e^{i\phi}|^2,\\ &=\frac{1}{2}\,(|r_{ss}|^2+r_{ss}^*(r_{sp}+\epsilon r_{pp})e^{-i\phi}\\ &\quad+r_{ss}(r_{sp}^*+\epsilon r_{pp}^*)e^{i\phi}), \end{aligned} \tag{16}$$

where * signifies the complex conjugate. We therefore obtain the normalized intensity

$$\begin{aligned} \frac{I}{I_{\rm dc}}&=1+4J_2\cos 2\omega t\ \mathrm{Re}\left(\frac{(r_{sp}+\epsilon r_{pp})}{r_{ss}}\right)\\ &\quad-4J_1\sin\omega t\ \mathrm{Im}\left(\frac{(r_{sp}+\epsilon r_{pp})}{r_{ss}}\right)+\cdots, \end{aligned} \tag{17}$$

where ϕ is the retardation angle of the PEM ($\phi=A\cos\omega t$, with $A=137.8°$ and $f=2\pi\omega=50$ kHz) and $J_{1,2}$ are first- and second-order Bessel functions evaluated at 137.8°. A was selected to equal 137.8° in order to eliminate the zeroth component of the Bessel function, which would have added a small contribution to the dc value of the signal.[12]

The output of the lock-in amplifier at ω is therefore proportional to the imaginary part of $(r_{sp}+\epsilon r_{pp})/r_{ss}$, while the output at 2ω is proportional to the real part of $(r_{sp}+\epsilon r_{pp})/r_{ss}$. Because the quantity ϵr_{pp} changes very little with the applied magnetic field in comparison to r_{sp}, the height of the measured magneto-optic hysteresis loop is equal to $2\times(r_{sp}/r_{ss})$ and the term ϵr_{pp} represents merely an offset in the overall rotation and ellipticity. The constants of proportionality were determined by a calibration procedure: at each photon energy, the analyzer was rotated by a total of 2° ($\epsilon=1°\rightarrow3°$) in increments and the observed response at 2ω fitted to a straight line to obtain a volts per degree rotation calibration factor. This factor had to be multiplied by the ratio of the s to p reflectivities to obtain the true rotation. This can be understood by noting that at Brewster's angle, where $r_{pp}=0$, the reflected wave will be entirely s polarized and will not undergo intensity reduction to first order as ϵ is changed. The calibration of the response at ω was accomplished in the same manner as that at 2ω, but with the addition of a rhombohedral prism (a broadband quarter wave plate) after the PEM in the optical path. Note that our measurements do not give us the traditional rotation and ellipticity as defined by Metzger, which are the real and imaginary parts of r_{ps}/r_{ss} for incident s-polarized light, because the light falling on the sample was polarized 45° to the plane of incidence. Nevertheless, we will use the terms ''rotation'' and ''ellipticity'' to signify the real and imaginary parts of r_{sp}/r_{ss}, respectively. The division by $I_{\rm dc}$ was performed experimentally by dividing by the dc output of the photodiode, which was amplified separately from its ac output. The dc signal normalization corrects for fluctuations in the incident intensity of the arc lamp.

To proceed, we need an expression for r_{sp}/r_{ss} that explicitly includes Q. Such an expression can be derived using the formalism of Zak *et al.*,[13] treating the Co underlayer as an infinitely thick layer covered by a nonmagnetic capping layer of thickness d and expanding to first order in Q (terms second order in Q go to zero for **M** saturated along the longitudinal direction).[7] In this case, r_{sp}/r_{ss} is given by

$$\begin{aligned} \frac{r_{sp}}{r_{ss}}&=\frac{iQm_l\cos\theta\,\sin\theta}{\gamma_0'}\,\frac{1}{(-\gamma_0'\cos\delta+i\gamma n_0'\sin\delta/n_0+(-n_0'\cos\delta+i\gamma_0'n_0\sin\delta/\gamma_0)\cos\theta)}\\ &\quad\times\frac{1}{(\gamma_0'n_0'\cos\delta+(-i)\gamma_0n_0\sin\delta+(\cos\delta+-i\gamma_0'n_0'\sin\delta/\gamma_0n_0)\cos\theta)}\\ &\quad\times\left(\frac{[(-i\gamma_0'n_0'/\gamma_0n_0)\sin\delta+\cos\delta]\cos\theta+i\gamma_0n_0\sin\delta-\gamma_0'n_0'\cos\delta}{[(-i\gamma_0'n_0'/\gamma_0n_0)\sin\delta+\cos\delta]\cos\theta-i\gamma_0n_0\sin\delta+\gamma_0'n_0'\cos\delta}\right)^{-1}, \end{aligned} \tag{18}$$

TABLE II. The energy dependence of Q values for hcp Co (Ref. 2) and with **M** along two crystalline axes of an epitaxial $(1\bar{1}00)$-oriented hcp Co film (present study).

Energy (eV) hcp Co	Q' (a)	Q'' (a)	Q' **M**$\parallel[1\bar{1}20]$	Q'' **M**$\parallel[1\bar{1}20]$	Q' **M**$\parallel$[0001]	Q'' **M**$\parallel$[0001]
1.5	0.0305	−0.0114	0.047	0.002	0.046	0.003
1.6	0.0268	−0.0087	0.043	0.002	0.041	0.003
1.7	0.0238	−0.0070	0.039	0.000	0.039	0.002
1.8	0.0214	−0.0058	0.038	−0.001	0.037	0.001
1.9	0.0201	−0.0051	0.036	−0.001	0.034	0.001
2.0	0.0189	−0.0043	0.038	−0.003	0.033	0.000
2.1	0.0183	−0.0037	0.036	−0.003	0.029	0.001
2.2	0.0176	−0.0031	0.035	−0.004	0.029	0.001
2.3	0.0168	−0.0023	0.033	−0.005	0.028	0.001
2.4	0.0159	−0.0016	0.032	−0.006	0.027	0.001
2.5	0.0150	−0.0012	0.030	−0.008	0.025	0.002
2.6	0.0140	−0.0008	0.028	−0.006	0.024	0.002
2.7	0.0133	−0.0005	0.027	−0.006	0.024	0.002
2.8	0.0125	−0.0004	0.026	−0.007	0.024	0.002
2.9	0.0118	−0.0003	0.026	−0.007	0.024	0.001
3.0	0.0111	−0.0004	0.025	−0.007	0.024	−0.001
3.2	0.0104	−0.0006	0.024	−0.005	0.022	−0.001
3.4	0.0114	−0.0006	0.024	−0.006	0.023	−0.002

[a]Reference 2.

where θ is the angle of incidence (36° in this case), n_0 is the index of refraction of the capping layer, n_0' and Q are the index of refraction and Q value of the magnetic material, γ_0 (γ_0') is the cosine of the angle between the transmitted wave in the capping (magnetic) layer and the surface normal, and $\delta=-2\pi n_0\gamma_0 d/\lambda$ is the phase delay of the wave as it crosses the capping layer (λ is the photon wavelength). The parameter m_l is the longitudinal component of **M**, normalized to the absolute value of **M** (i.e., the dimensionless component of **M** parallel to the plane of incidence); **M** was saturated to lie parallel to H so that $m_l=1$. One sees that in the limit $\delta\rightarrow 0$ ($\cos\delta\rightarrow 1$), Eq. (18) reduces to

$$\frac{r_{sp}}{r_{ss}}(\delta=0)=-\frac{iQm_l\cos\theta\,\sin\theta}{\gamma_0'}\times\frac{1}{(\gamma_0'\cos\delta+n_0'\cos\theta)(\gamma_0'n_0'+\cos\theta)}\times\left(\frac{-n_0'\gamma_0'+\cos\theta}{n_0'\gamma_0'+n_0'\cos\theta}\right)^{-1}, \tag{19}$$

which is what one obtains using the standard bulk expressions for r_{sp} and r_{ss}.[7]

A spreadsheet program was used to calculate the coefficient of Q in Eq. (18) as a function of photon energy, from which it was possible to invert Eq. (18) and obtain Q. Zak *et al.* used a convention for the imaginary part of n_0 and Q that is opposite to that adopted here. Equation (18) takes this into account, so that δ has a sign opposite to that given by Zak *et al.*[13]

The real and imaginary parts of r_{sp}/r_{ss} were measured as a function of photon energy. At each energy, the rotation and ellipticity were first calibrated by rotating the analyzer by 2° and fitting the observed response to a straight line in order to get a reading of volts per degrees rotation. For the ellipticity calibration, the beam passed through a rhombohedral prism, which acts as a broadband quarter wave plate.

Indices of refraction for the polycrystalline Co sample were determined with a commercial ellipsometry system. The ellipsometric angles (ψ and Δ) were measured as a function of wavelength at three different angles of incidence to fit for the indices of refraction. The resulting indices of refraction, along with those given by KA, are given in Fig. 5.

IV. RESULTS

A. hcp Co

Figure 6(a) displays the resulting Q values for the hcp Co sample. Also plotted in Fig. 6(a) are the values obtained by KA for a polycrystalline Co sample. There are significant differences in the Q values obtained with **M** along [0001] and $[1\bar{1}20]$ (the c and a axes, respectively), particularly in the range 2–3 eV. Note that KA's Q values, which were measured from polycrystalline Co plates, do not fall between our values for the [0001] and $[1\bar{1}20]$ directions. Therefore, the discrepancy between our values and KA's cannot be explained by anisotropy alone. Our values for Q' are more positive than those of KA, while our value of Q'' has the opposite sign from that of either KA or Weller *et al.* for small energies, in agreement with the results of Qiu, Pearson, and Bader (note that we use a different sign convention than these authors)[3] and Prinz *et al.*[14] Our differences with KA could be due to either of two factors: (1) inconsistencies in their experiment (of order 10–20 % as estimated from Fig. 8 of their article[2]) and/or (2) the presence of a thin oxide layer on their samples (see below). Virtually the same indices of

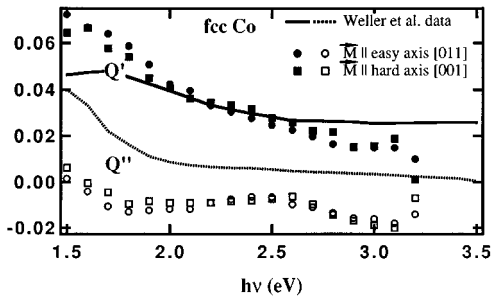

FIG. 7. Q values as a function of photon energy ($h\nu$) for the fcc Co sample. The black (clear) circles are Q' (Q'') **M** along the in-plane [011] direction (easy axis); indices of refraction are from the polycrystalline Co sample. The solid (clear) boxes is Q' (Q'') for **M** along the in-plane [001] direction (hard axis); indices of refraction are from the polycrystalline sample. The solid (dotted) lines are Q' (Q'') from the data of Weller *et al.* (Ref. 4), using indices of refraction from KA (Ref. 2).

refraction were used for extracting Q values from all three studies (see Fig. 5), we can rule out the possibility that the differences in the Q values were due to an artifact of the data analysis (i.e., dividing the observed magneto-optic response by different indices of refraction).

Our results are in qualitative agreement with those of Weller *et al.*, who reported the rotation and ellipticity for hcp Co with **M** either along [0001] or [1120].[4] Weller *et al.* prepared epitaxial Co films with either of these directions normal to the film plane, and then pulled **M** out-of-plane with an applied field of 20 kOe. The values of Q extracted from their data are displayed in Fig. 6(b) Weller *et al.* obtained Q' values similar to ours, and also reported positive values for Q'' at low energies, in contrast with our results and those of Ref. 3. They also obtained the same anisotropy in Q as us [Fig. 6(b)] with Q' and Q'' being more positive for **M** parallel to the [1120] and [0001] directions, respectively, in the energy range 2–3 eV. For both the results in Figs. 6(a) and 6(b), the anisotropy in both Q' and Q'' reaches a maximum of ~0.01 in this region. This agreement confirms Weller's conclusion that the magneto-optic response for **M** parallel to different crystallographic directions in hcp Co is not due to optical differences between samples, but rather is inherent to the spin-orbit interaction in the hcp crystal lattice.

One can obtain a sense of how the Q value (extrapolated from the magnetooptic response) depends on the presence of a thin, nonmagnetic capping layer, such as the Cr layer used for our samples or a surface oxide on uncapped samples. One must compare the Q values for a fixed magneto-optic response found with and without d in Eq. (18) set to zero. The results of such an analysis, for the hcp Co sample with **M** along the [0001] direction, are given in Fig. 6(c). The effect of the Cr capping layer is to shift Q' (Q'') towards more positive values by ~0.005 at all energies (Q'' is affected less by the capping layer at large energies). Such shifts in Q' and Q'' due to the presence of the capping layer might provide a clue as to the discrepancies in the literature about the sign of Q'' at $\lambda = 6328$ Å.[3] The Q values for the hcp sample appear in Table II.

TABLE III. The energy dependence of Q values for fcc Co from Ref. 4 (**M** along [001] and [011] gives virtually identical results) and with **M** along two crystalline axes of an epitaxial (100)-oriented fcc Co film (present study).

Energy (eV) fcc Co	Q' (a)	Q'' (a)	Q' **M**∥[001]	Q'' **M**∥[001]	Q' **M**∥[011]	Q'' **M**∥[011]
1.5	0.041	0.023	0.064	0.007	0.073	0.002
1.6	0.038	0.019	0.068	0.000	0.067	−0.003
1.7	0.037	0.016	0.058	−0.003	0.065	−0.010
1.8	0.036	0.012	0.057	−0.010	0.060	−0.013
1.9	0.035	0.009	0.046	−0.008	0.055	−0.013
2.0	0.034	0.008	0.043	−0.009	0.042	−0.011
2.1	0.033	0.006	0.037	−0.009	0.043	−0.013
2.2	0.031	0.005	0.035	−0.009	0.035	−0.010
2.3	0.030	0.004	0.034	−0.009	0.031	−0.008
2.4	0.028	0.004	0.033	−0.008	0.030	−0.007
2.5	0.028	0.003	0.031	−0.008	0.026	−0.006
2.6	0.027	0.003	0.026	−0.007	0.024	−0.007
2.7	0.026	0.001	0.026	−0.006	0.022	−0.011
2.8	0.026	0.001	0.021	−0.011	0.019	−0.011
2.9	0.026	0.001	0.022	−0.015	0.016	−0.014
3.0	0.026	0.001	0.014	−0.017	0.015	−0.016
3.2	0.026	0.000	0.019	−0.021	0.015	−0.018

[a]Reference 4.

B. fcc Co

Figure 7 displays the results obtained from the epitaxial fcc Co(100). The Q values for **M** parallel to the [001] and [011] directions [the hard (ha) and easy (ea) axes, respectively] are plotted as circles and boxes, respectively. Also displayed in Fig. 7 are the Q values for fcc Co extracted from the results of Weller *et al.* (curves).[4]

TABLE IV. The energy dependence of the index of refraction (n,k) for polycrystalline Co determined by a commercial ellipsometry system.

Energy (eV)	n	k
1.40	2.19	4.01
1.50	2.79	4.78
1.60	2.66	4.59
1.70	2.54	4.43
1.80	2.41	4.27
1.90	2.30	4.14
2.00	2.19	4.01
2.10	2.09	3.89
2.20	1.99	3.77
2.30	1.90	3.65
2.40	1.82	3.54
2.50	1.74	3.44
2.60	1.67	3.33
2.70	1.60	3.23
2.80	1.53	3.13
2.90	1.48	3.03
3.00	1.43	2.94
3.20	1.34	2.94
3.40	1.28	2.58

The Q values for the easy and hard axes are very close, as anticipated. Because the magneto-optic response is fourth order in the spin-orbit interaction for fcc Co, but second order in the spin-orbit interaction for hcp Co, the anisotropy in the Kerr effect should be much smaller for fcc Co, in agreement with our results and those of Ref. 4. There are some differences between the Q values for **M** parallel to the [001] and [011] directions; however, these differences are readily attributed to scatter in the data and not the result of anisotropy. At 2.0 eV, Q'' is negative, in agreement with Qiu, Pearson, and Bader and in disagreement with Weller *et al.*[3,4] The Q values for the fcc sample appear in Table III.

One important point to be considered is the appropriate indices of refraction for both the fcc and hcp samples. When we used the KA indices of refraction, we obtained Q values very similar to those obtained when we used our own indices measured on our own samples. Differences in the Q values calculated in this manner were $\sim$10% at $h\nu<1.7$ eV and $<$5% at higher energies (see Table IV).

In extracting Q values from the rotation and ellipticity data of Weller *et al.*,[4] we have multiplied their ellipticity values by -1 to account for the sign in Eq. (12). We checked that a sign error will not cause Q'' to be negative at low energies. In addition, a sign change in our ellipticities does not produce a positive Q'' at low energies. The quantitative difference in the sign of Q'' remains an issue, and it is clear that it cannot be explained by anisotropy alone (i.e., our measurements being made with **M** along a different crystalline axis than those in Ref. 4). We note that the samples used by Weller *et al.*[4] were uncapped, which may have produced a thin oxide layer on top of their sample, shifting their Q values in the sense of Fig. 6(c).

V. CONCLUSIONS

We have tabulated the wavelength dependence of the complex magneto-optic constant (Q) for epitaxial fcc and hcp Co with **M** along two different in-plane crystallographic directions. The Q values of hcp Co were found to be significantly anisotropic, in contrast to those for fcc Co. This is in agreement with the results of Weller *et al.*[4] obtained on samples with different crystallographic directions aligned out-of-plane. It is also consistent with simple arguments based on the spin-orbit interaction. Our values for Q'' are negative at low energy, in contrast to those reported by Weller *et al.*[4] and KA,[2] but in agreement with Qiu, Pearson, and Bader at $\lambda=6328$ Å.[3] Our values for the anisotropy of Q in hcp Co agree quantitatively with that reported by Weller *et al.*, reaching a maximum of $\sim$0.01 in the energy 2–3 eV. The quantitative discrepancies between Q values in the literature cannot be explained by the anisotropy in Q, but may be due to a thin surface oxide.

ACKNOWLEDGMENTS

We acknowledge useful discussions with Eric Fullerton and D. Weller. This work was supported by the U.S. Department of Energy, Basic Energy, Sciences-Materials Sciences under Contract No. W-31-109-ENG-38.

*Permanent address: Physics Department, Stetson University, DeLand, FL 32720.

†Present address: Physics Department, Georgia State University, Atlanta, GA 30303.

‡Present address: Motorola, Inc. 1301 Algonquin Rd. Schaumburg, IL 60196.

[1] E. R. Moog and S. D. Bader, Superlattices Microstruct. **1**, 543 (1985).

[2] G. S. Krinchik and V. A. Artem'ev, Sov. Phys. JETP **26**, 1080 (1968).

[3] Z. Q. Qiu, J. Pearson, and S. D. Bader, Phys. Rev. B **46**, 8195 (1992).

[4] D. Weller, G. R. Harp, R. F. C. Farrow, A. Cebollada, and J. Sticht, Phys. Rev. Lett. **72**, 2097 (1994).

[5] G. A. Bolotin and A. V. Sokolov, Fiz. Met. Metalloved. **12**, 493 (1961); **12**, 625 (1961); **12**, 785 (1961).

[6] E. M. Pugh and N. Rostoker, Rev. Mod. Phys. **25**, 151 (1953).

[7] G. Metzger, P. Pluvinage, and R. Torguet, Ann. Phys. (Paris) **10**, 5 (1965).

[8] W. Reim and J. Schoenes, in *Ferromagnetic Metals*, edited by K. H. J. Buschow and E. P. Wohlfarth (Elsevier, Amsterdam, 1990), Vol. 5, p. 133.

[9] M. Grimsditch, Eric E. Fullerton, and R. L. Stamps, Phys. Rev. B **56,** 2617 (1997).

[10] CVI Instruments, Albuquerque, New Mexico, 87123: focal length of 24 cm, wavelength resolution of approximately 1 nm.

[11] E. Hecht and A. Zajac, *Principles of Optics* (Addison-Wesley, Reading, MA, 1979).

[12] K. Sato, J. Phys. Soc. Jpn. **20**, 2403 (1981).

[13] J. Zak, E. R. Moog, C. Liu, and S. D. Bader, J. Magn. Magn. Mater. **89**, 107 (1990).

[14] G. A. Prinz, J. J. Krebs, D. W. Forester, and W. G. Maisch, J. Magn. Magn. Mater. **15-18**, 779 (1980).